# Interaction of Typhoon and Mesoscale Vortex

CHEN Lianshou*[1] (陈联寿) and LUO Zhexian[2] (罗哲贤)

[1] *Chinese Academy of Meteorological Sciences, Beijing* 100081

[2] *Nanjing Institute of Meteorology, Nanjing* 210044

(Received 19 May 2003; revised 11 February 2004)

**ABSTRACT**

Under two types of initial tropical cyclone structures that are characterized by high and low vorticity zones, four sets of numerical experiments have been performed to investigate the interaction of a tropical cyclone with an adjacent mesoscale vortex (MSV) and its impact on the tropical cyclone intensity change, using a quasi-geostrophic barotropic vorticity equation model with a horizontal resolution of 0.5 km. The results suggest that the interaction of a tropical cyclone characterized by a high vorticity zonal structure and an MSV would result in an intensification of the cyclone. Its central pressure decreases by more than 14 hPa. In the process of the interaction, the west and middle segments of the high vorticity zone evolve into two peripheral spiral bands of the tropical cyclone, and the merging of the east segment and the inward propagating MSV forms a new vorticity accumulation area, wherein the maximum vorticity is remarkably greater than that in the center of the initial tropical cyclone circulation. It is this process of merging and strengthening that causes a greater pressure decrease in the center of the tropical cyclone. This process is also more complicated than those that have been studied in the past, which indicated that only the inward transfer of vorticity of the MSV can result in the strengthening of the tropical cyclone.

**Key words:** tropical cyclone structure, intensity change, vortex Rossby wave

## 1. Introduction

There are large differences in landfalling tropical cyclones in China. Some of them will quickly dissipate right after they make landfall, while others will be sustainable over land for a long period. Chen and Ding (1979) pointed out that one possible mechanism for a landfalling tropical cyclone to sustain itself over land is the interaction with the adjacent mesoscale vortex (MSV), especially when the MSV, merges into a tropical cyclone.

With regard to the dynamics of the interaction of a tropical cyclone with its adjacent MSV, researchers have made certain contributions. In terms of a barotropic model, using a stationary tropical cyclone circulation with an MSV at its maximum wind radius as the initial field, Möller and Montgomery (MM hereafter, 1999) demonstrated that the inward propagation, in a manner of vortex Rossby waves (VRW), of the relative vorticity of the MSV leads to the increase in the mean tangential velocity at 90 km in the inner region from the center of tropical cyclone.

On the other hand, there are three relevant problems that need to be further investigated. First, a stationary tropical cyclone circulation assumption was used in MM; that means that there is the effect of the tropical cyclone on the MSV but no influence of the MSV on the tropical cyclone. Second, in the real atmosphere, the interaction of the tropical cyclone and MSV sometimes results in the intensification of tropical cyclone, but sometimes it may not. The question is how to distinguish the one from the other. Third, is there a distinct intensification in mean tangential velocity?

This paper presents new results for the three problems.

## 2. Model and experiments

In the numerical studies on VRW propagation, the f-plan assumption is generally used. By now, the quasigeostrophic barotropic model equation has the following form:

$$\frac{\partial \nabla^2 \psi}{\partial t} + J(\psi, \nabla^2 \psi) = 0 \,, \qquad (1)$$

*E-mail: cams@public.bta.net.cn

where $\psi$ is the geostrophic stream function. The computational domain is a square of 200 km×200 km with its median on $\phi_0 = 25°$N. The grid spacing is 0.5 km, amounting to 401×401 grid points in total, $i = 1, 2, \ldots, 401$ and $j = 1, 2, \ldots, 401$ which increase eastwards and northwards respectively, the time step is 10 seconds.

$\partial\psi/\partial t = 0$ on the south/north boundaries; the cyclic boundary condition is used on the east/west boundaries.

With regard to the initial condition, set

$$\xi(x, y, 0) = \overline{\xi}(x, y, 0) + \xi'(x, y, 0) \,, \tag{2}$$

where $\overline{\xi}$ and $\xi^{'}$ denote the initial vorticity fields of the tropical cyclone vortex and MSV respectively. The initial vorticity field, $\overline{\xi}(x, y, 0)$, of the tropical cyclone is given by the following formula (Kossin and Schubert, 2001):

$$\overline{\xi}(x,y,0) = \begin{cases} \xi_1 \,, & 0 \leqslant r < r_1 \\ \xi_1 S[(r-r_1)/(r_2-r_1)] + \xi_2 S[(r_2-r)/(r_2-r_1)] \,, & r_1 \leqslant r < r_2 \\ \xi_2 S[(r-r_2)/(r_3-r_2)] + \xi_1 S[(r_3-r)/(r_3-r_2)] \,, & r_2 \leqslant r < r_3 \\ \xi_1 \,, & r_3 \leqslant r < r_4 \\ \xi_1 S[(r-r_4)/(r_3-r_4)] + \xi_3 S[(r_5-r)/(r_5-r_4)] \,, & r_4 \leqslant r < r_5 \\ \xi_3 \,, & r_5 \leqslant r \,, \end{cases} \tag{3}$$

where $\xi_1$ , $\xi_2$ are the given vorticity parameters; $\xi_1 > 0$ , $\xi_2 > 0$. $\xi_3$ is an undetermined parameter, $\xi_3 < 0$. The value of $\xi_3$ is determined according to the following regulation: its sum over the grids of the whole computational domain is zero. $S(p) = 1 - 3p^2 + 2p^3$ is the Hermite shape function, and $p$ is a parameter of the function, $r = \sqrt{(x-x_0)^2 + (y-y_0)^2}$, where $(x_0, y_0)$ are the coordinates of the center of the initial tropical cyclone vortex. $r_k$ $(k = 1, 2, \cdots, 5)$ is a given radial distance parameter.

The initial vorticity field, $\xi'(x, y, 0)$ of the MSV is given by the following expression (Ohnishi, 1991):

$$\xi'(x, y, 0) = \frac{d^2\psi'}{dq^2} + \frac{1}{q}\frac{d\psi'}{dq} \tag{4}$$

$$\psi'(x, y, 0) = \psi_0[1 - (q/q_0)^2]^n \,, \tag{5}$$

where $\psi'(x, y, 0)$ is the perturbation stream function field of the initial MSV, $q = \sqrt{(x-x_q)^2 + (y-y_q)^2}$, $(x_q, y_q)$ are the coordinates of the center of the initial MSV. $q_0$ is the radius of the initial MSV. $\psi_0$ and $n$ are given parameters, and describe the intensity and structure of the initial MSV respectively. When $n = 4$, it is a tight vortex (Ohnishi, 1991).

Four sets of experiments are performed for two model hours.

In Experiment 1, there is only a tropical cyclone vortex in the initial field, and its parameters are given as $(r_1, r_2, r_3, r_4, r_5) = (8, 14, 20, 30, 40)$ km; $(\xi_1, \xi_2, \xi_3) = (1.0, 31.25, -0.77) \times 10^{-4}$ s$^{-1}$. The coordinates of the center of the tropical cyclone are $(I_0, J_0) = (201, 201)$, i.e., the center of the computational domain. The maximum wind radius $r_{\rm m1}$ of the tropical cyclone is about 21 km.

In Experiment 2, there is a tropical cyclone vortex and an MSV in the initial field. Parameters of the tropical cyclone vortex are the same as those in Experiment 1. The center, $(I_q, J_q) = (232, 170)$, of the initial MSV lies at the maximum wind radius about 21 km southeast of the tropical cyclone center, $\psi_0 = -1.4 \times 10^5$ m$^2$ s$^{-1}$.

In Experiment 3, there is only a tropical cyclone vortex in the initial field, and its parameters are given as $(r_1, r_2, r_3, r_4, r_5) = (8, 10, 12, 30, 40)$ km; $(\xi_1, \xi_2, \xi_3) = (1.0, 250.0, -0.94) \times 10^{-4}$ s$^{-1}$. The coordinates of the center of the tropical cyclone are $(I_0, J_0) = (201, 201)$, and the maximum wind radius, $r_{\rm m2}$, of the tropical cyclone is about 10.5 km.

In Experiment 4, there is a tropical cyclone vortex and an MSV in the initial field. The parameters of the tropical cyclone vortex are the same as those in Experiment 3. The position, structure, and intensity of the initial MSV are the same as in Experiment 2, and the center of the MSV lies at $2r_{\rm m2}$.

In Experiments 1 and 2, the maximum value of the initial tropical cyclone vorticity fields is $\overline{\xi}_{\rm max}$=31.25×10$^{-4}$ s$^{-1}$ (Fig. 1a), the maximum tangential velocity $\overline{V}_{\rm max}$ is 17.9 m s$^{-1}$, and the radius of maximum wind is $r_{\rm m1}$=21 km. The tangential velocity increases slowly over the interval of 10.0 km $< r <$ 21.0 km (Fig. 1b).

In Experiments 3 and 4, the maximum value of the initial tropical cyclone vorticity field is $\overline{\xi}_{\rm max}$=250.0×10$^{-4}$ s$^{-1}$ (Fig. 1c) which is 8 times of that in Experiments 1 and 2; $\overline{V}_{\rm max}$=42.6 m s$^{-1}$, $r_{\rm m2}$=10.5 km. The tangential velocity increases rapidly over the interval of 8.0 km $< r <$ 10.5 km (Fig. 1d).

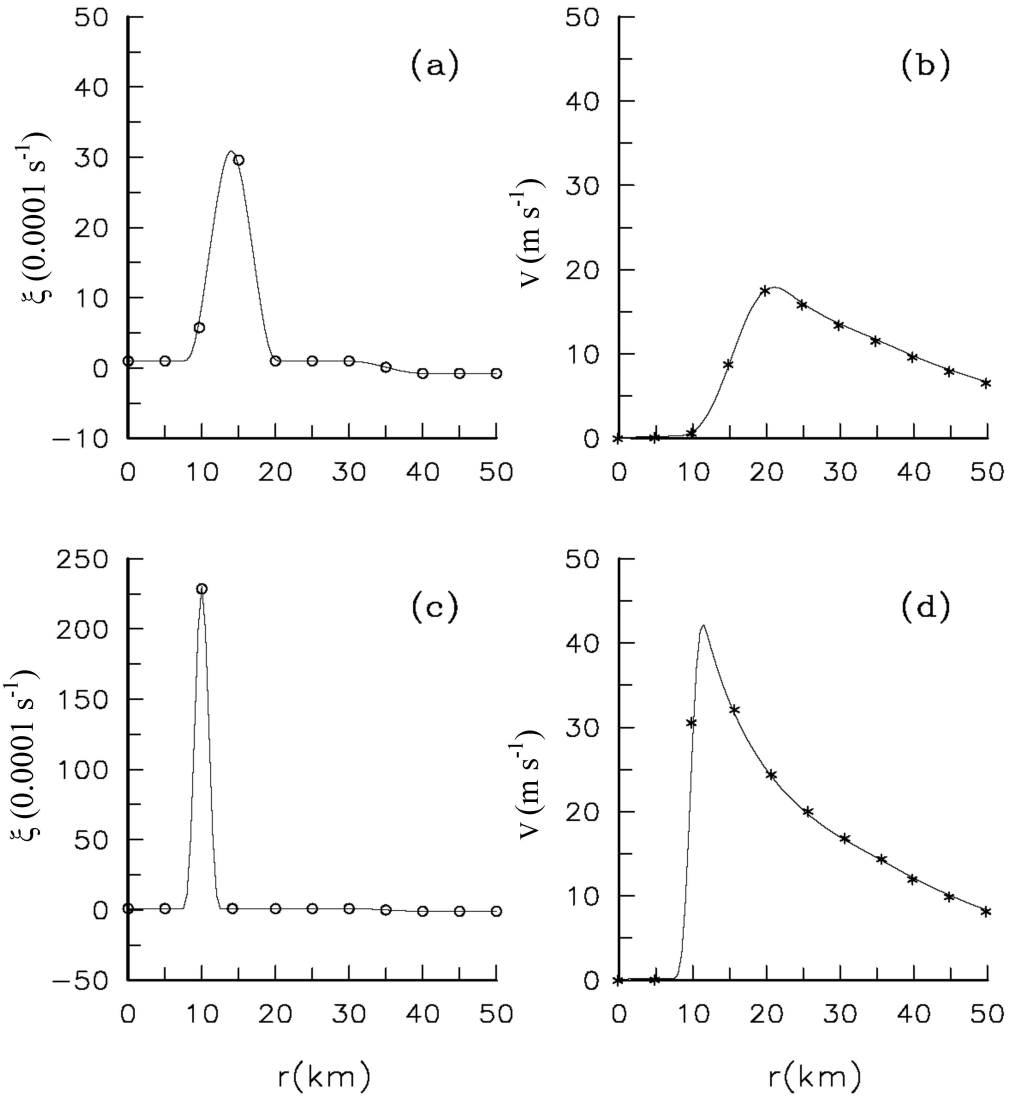


**Fig. 1.** Vorticity, $\xi(r)$, and tangential velocity, $\overline{V}(r)$, profiles of initial tropical cyclones in Expts. 1–4 (a–d respectively).

In Experiment 1, the initial tropical cyclone circulation is stable, and there exists only the advection of the relative vorticity of the tropical cyclone circulation. In Experiment 2, there exists the interaction of the tropical cyclone and the adjacent MSV. In Experiment 3, the initial tropical cyclone circulation is unstable. Before destablization, there exists the advection of the relative vorticity of tropical cyclone circulation; after destablization, there exists the interaction of the tropical cyclone circulation with multiple small vortices. In Experiment 4, there exists the interaction between the initial unstable tropical cyclone circulation and the adjacent MSV.

The distribution of initial vorticity fields, $\xi(x, y, 0)$, is given in Fig. 2. Obviously, $\xi(x, y, 0)$ in Experiments 1 and 2 shows a pattern of low vorticity zonal structure of a tropical cyclone (Figs. 2a, 2b), while $\xi(x, y, 0)$ in Experiments 3 and 4 exhibits a pattern of high vorticity zonal structure of a tropical cyclone (Figs. 2c, 2d). These are two different radial structures of a tropical cyclone. In Experiments 2 and 4 (Figs. 2b and 2d), a MSV with a maximum tangential velocity of 26.8 m $s^{-1}$ is introduced.

Based on the results of the four experiments performed under conditions of the two types of tropical cyclone structures, the interaction between the tropical cyclone and MSV and its effect on the tropical cyclone intensity changes can be analyzed.

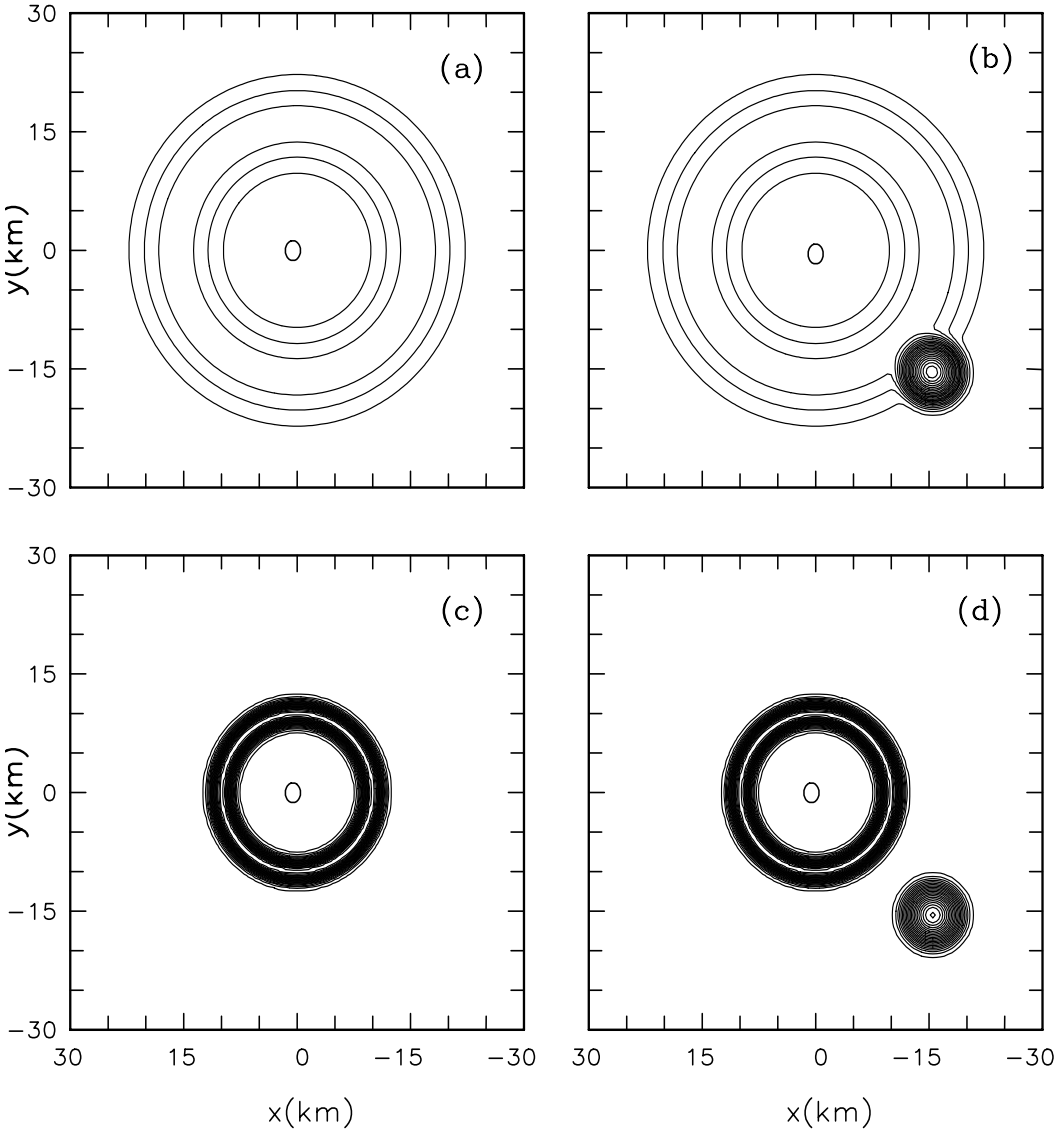


**Fig. 2.** Distributions of initial vorticity field, $\xi(x, y, 0)$, in Experiments 1 (a), 2 (b), 3 (c), and 4 (d). Point O denotes the position of the tropical cyclone center. The contour interval is $10.0\times10^{-4}$ $s^{-1}$, and the outermost and innermost contours of the tropical cyclone vortex are $5.0\times10^{-4}$ $s^{-1}$ in (a) and (c).

The quasigeostrophic barotropic model outputs the gridded (401×401) vorticity field $\xi(x, y)$ every 10 minutes of integration, therefore $\psi(x, y)$ is derived. Then the nonlinear balance equation

$$\frac{1}{\rho}\nabla^2 p(x,y) = f\nabla^2\psi + 2\left[\frac{\partial^2\psi}{\partial x^2}\frac{\partial^2\psi}{\partial y^2} - \left(\frac{\partial^2\psi}{\partial x\partial y}\right)^2\right] \quad (6)$$

is used to calculate $p(x, y)$ under the assumptions of $\rho = 1.13$ kg m$^{-3}$ and $p_{\sum} = 0.0$ on the boundaries $\sum$ of the computational domain. $\rho$ is the air density, $p(x, y)$ describes the pressure distribution relative to that on the boundary, therefore it is called the relative pressure field hereafter.

We are going to analyze changes in the intensity of the tropical cyclone in terms of the relative pressure field $p(x, y)$ and the relative pressure $p_0$ at the center of the tropical cyclone.

## 3. Interaction of tropical cyclone and mesoscale vortex under the condition of low vorticity zonal structure

In Experiment 1, there is only an initial tropical

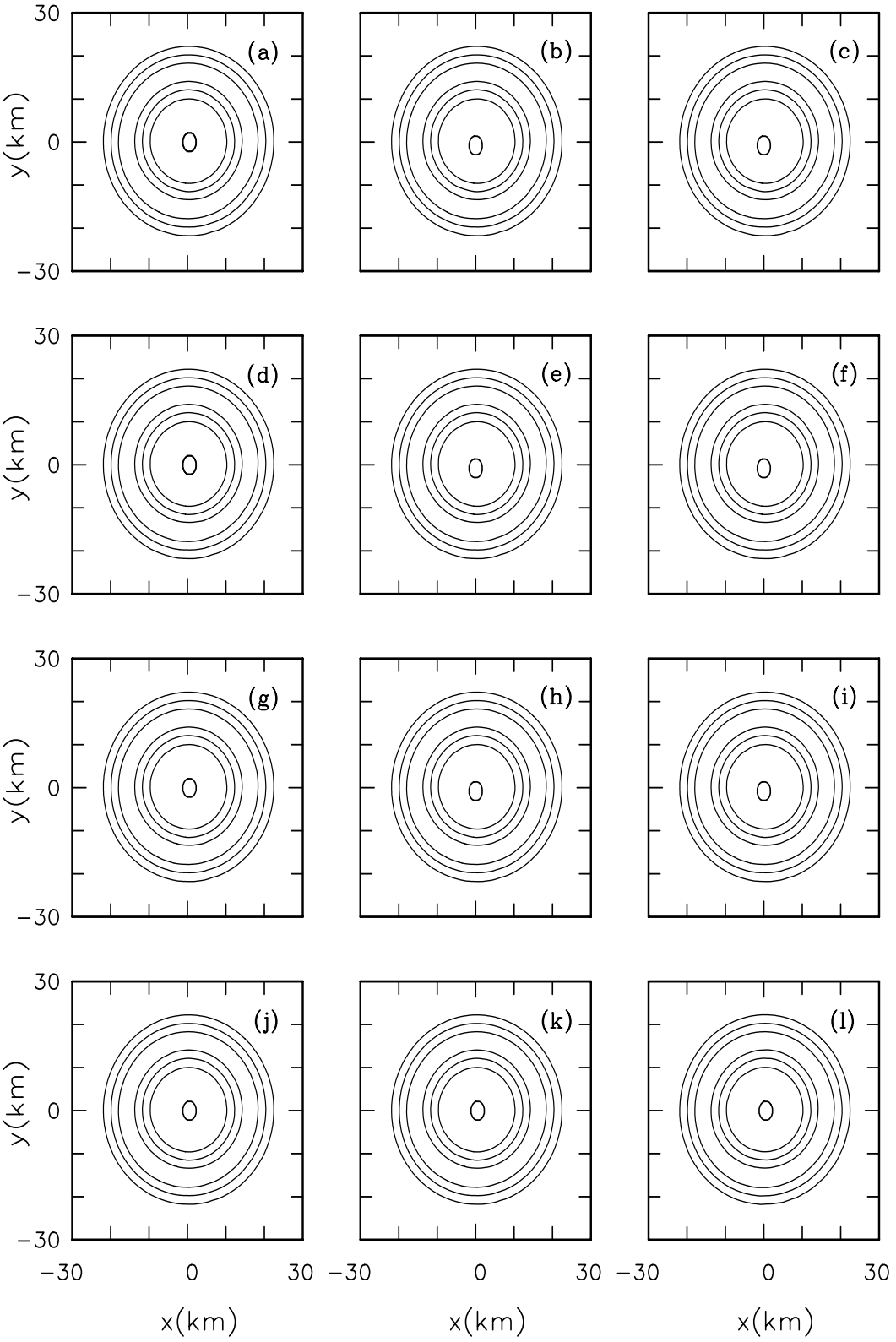


**Fig. 3.** Temporal changes of the vorticity field $\xi(x, y)$ in Expt. 1 at $t = 0$ (a), 10 (b), 20 (c), $\cdots$, 110 (l) min. The contour interval is $10.0\times10^{-4}$ s$^{-1}$, and point O denotes the position of the tropical cyclone center. The panel area given is 60 km×60 km, while the real computed area is 200 km×200 km.

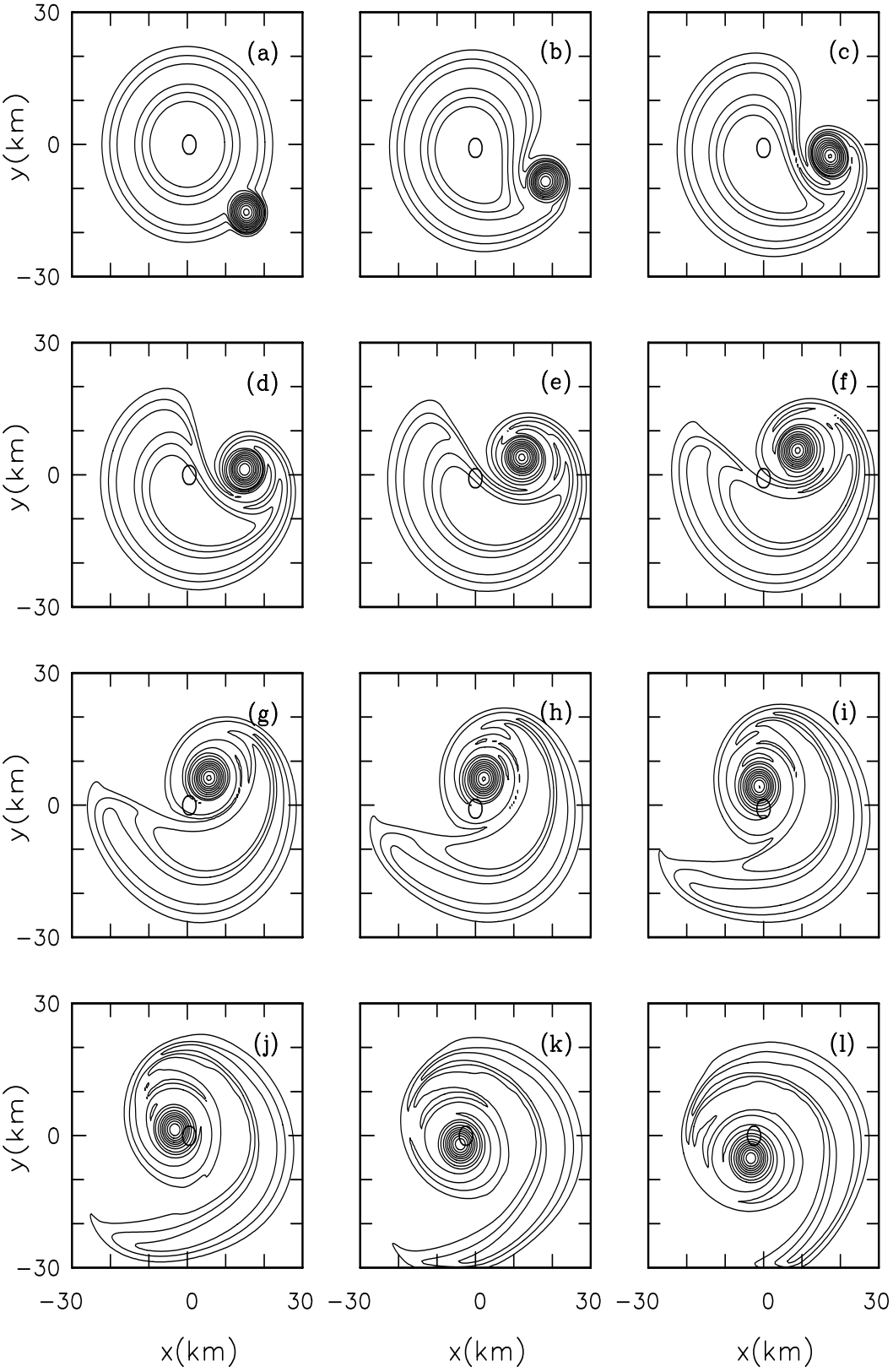


**Fig. 4.** Same as Fig. 3 except for Expt. 2.

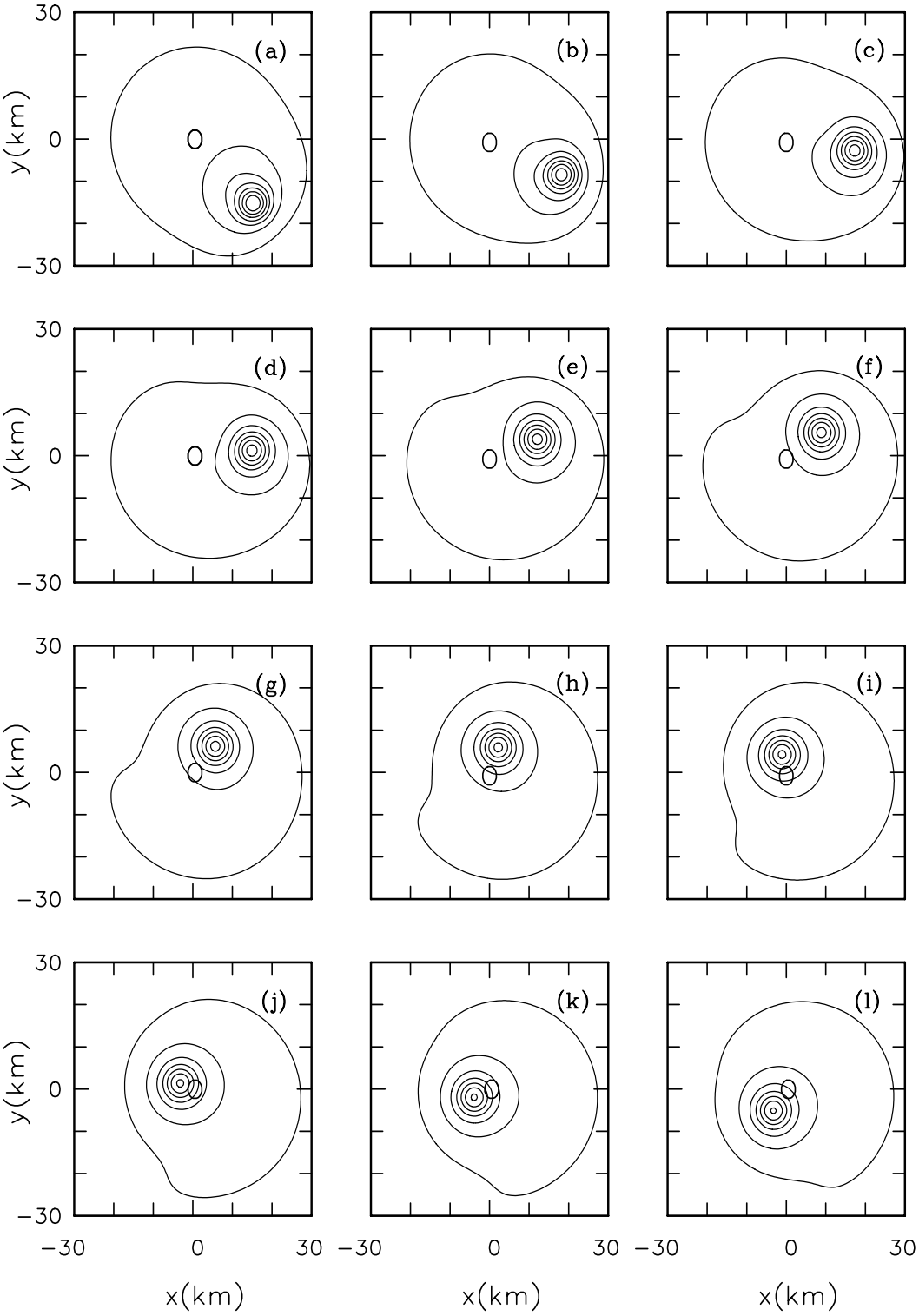


**Fig. 5.** Temporal changes of the relative pressure field $p(x, y)$ in Expt. 2 at $t = 0$ (a), 10 (b), 20 (c), $\cdots$ , 110 (l) min. The contour interval is 2.0 hPa, and the others are the same as Fig. 3.

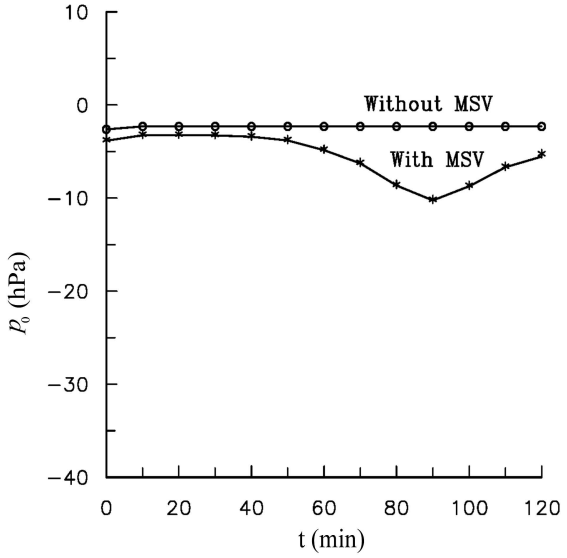


**Fig. 6.** Temporal variations of the tropical cyclone central relative pressure ($p_0$) in Expt. 1 (circles) and 2 (stars).

cyclone vortex without an MSV, and it has a low vorticity zonal structure. The temporal change of the vorticity field $\xi(x, y)$ is not evident (Fig. 3).

The pressure is relatively uniform, and the tangential velocity is very small (Fig. 1b) in the region of $r < 10$ km in the initial relative pressure field $p(x, y)$ of Experiment 1. The isobars are concentrated near $r = 20$ km, and the corresponding tangential velocity is increased (Fig. 1b). The temporal changes of the relative pressure pattern are also not obvious.

In Experiment 2, a tropical cyclone vortex and an MSV coexist in the initial vorticity field (Fig. 4a). When $t = 0$, the center of the MSV is located 21 km southeast of the tropical cyclone center (Fig. 4a); at $t = 30$ min, the center lies at 15 km due east of the tropical cyclone center (Fig. 4d); and at $t = 70$ min, the center is 6 km almost due north of the tropical cyclone center (Fig. 4h). This means that under the steering of the tropical cyclone circulation, the MSV rotates anticlockwise and approaches the point O, i.e., the initial position of the tropical cyclone center. After $t = 70$ min, the MSV continues to approach to the point O, and when $t = 90$ min (Fig. 4j), the center of the MSV almost coincides with the point O. Then the MSV departs slightly from the point O afterwards (Figs. 4k and 4l).

When $t = 0$, the tropical cyclone vortex basically exhibits a circular pattern (Fig. 4a). Along with the anticlockwise rotation of the MSV, the circular tropical cyclone vortex deforms, and rotates anticlockwise, to exhibit a phenomenon of the mutual rotation of binary vortices (Figs. 4c–h). When $t = 90$ min (Fig. 4j), the center of the MSV has overlapped with the point O which is the initial position of tropical cyclone vortex, and the original tropical cyclone circulation has elongated, narrowed , and become a spiral vorticity band (Fig. 4j), forming a new typhoon-like flow pattern in which the MSV becomes a dominant part of the tropical cyclone to replace the original one (Figs. 4k–l).

The above process in which the MSV approaches the point O of the initial position of the tropical cyclone center is just the process of transferring the vorticity of the MSV onto the point O. Phenomenally, this inward propagation of vorticity increases the vorticity at point O to result in the increase of the tropical cyclone intensity.

The manner of motion in which the MSV rotates and approaches the point O is also clearly shown in the evolution process of the relative pressure $p(x, y)$ (Fig. 5). When $t = 0$, the relative pressure $p_0$ at the initial tropical cyclone center point O is about –2.0 hPa., and when $t = 50$ min, it drops to –3.0 hPa (Fig. 5f); when $t = 70$ min, $p_0$ is about –5.0 hPa (Fig. 5h), and when $t = 90$ min, it has decreased to about –9.0 hPa (Fig. 5j). $p_0$ slightly increases afterwards (Figs. 5k–l).

The temporal variations of $p_0$ in Experiments 1 and 2 (Fig. 6) indicate that the relative central pressure $p_0$ has almost no change with time if there is no interaction with the MSV (Experiment 1) and that the relative central pressure will be decreased obviously if there is interaction with an MSV (Experiment 2). It is shown in Experiment 2 that the maximum decrease of $p_0$ is –9.0 hPa at the time $t = 90$ min and the mean decrease of $p_0$ is –3.8 hPa in the period of $t = 40$ min to 120 min.

## 4. Interaction of tropical cyclone and mesoscale vortex under the condition of high vorticity zonal structure

In Experiment 3, there is only an initial tropical cyclone vortex without an MSV, and temporal variations of the vorticity field $\xi(x, y)$ (Fig. 7) are obviously different from those (Fig. 3) of the low vorticity zonal structure of a tropical cyclone.

At the initial time $t = 0$, the vorticity field shows a circular pattern (Fig. 7a), and at $t = 30$ min, it is approximately a rhombic pattern (Fig. 7d); when $t = 40$ min, the vorticity zone broadens, and its peripheral contours become unsmooth (Fig. 7e); at $t = 50$ min, the initially smooth circular vorticity zone splits into four closed centers that become the four vertexes of a quadrangle, and their peripheral contours are also unsmooth (Fig. 7f) showing the feature of a fracture(Luo, 1999). Because the high vorticity zone corresponds to

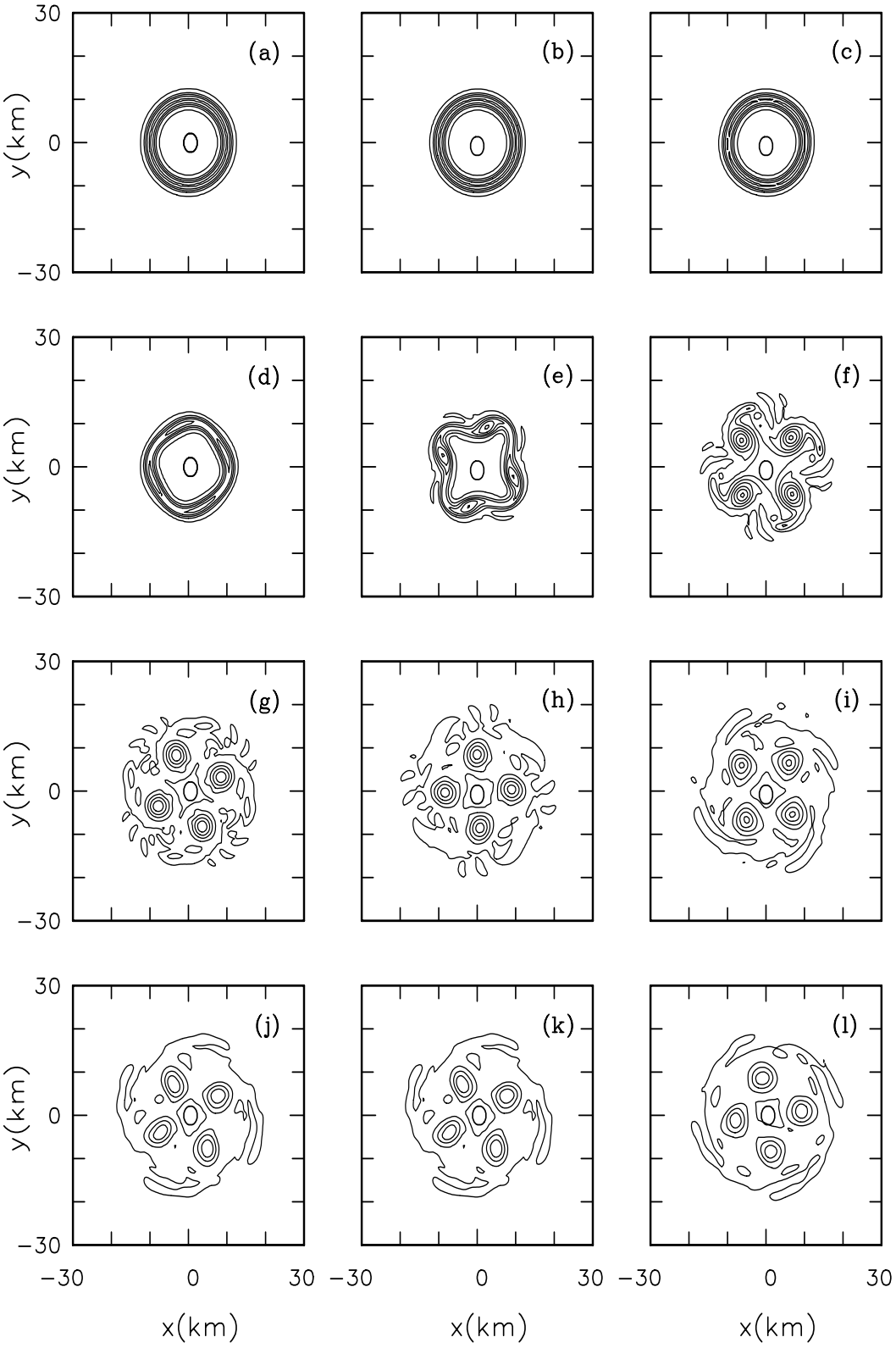


**Fig. 7.** Temporal changes of the vorticity field $\xi(x, y)$ in Expt. 3. The outmost peripheral contour of the vortex is $5.0 \times 10^{-4}\ \mathrm{s}^{-1}$, and the contour interval is $50.0 \times 10^{-4}\ \mathrm{s}^{-1}$. The others are the same as Fig. 3.

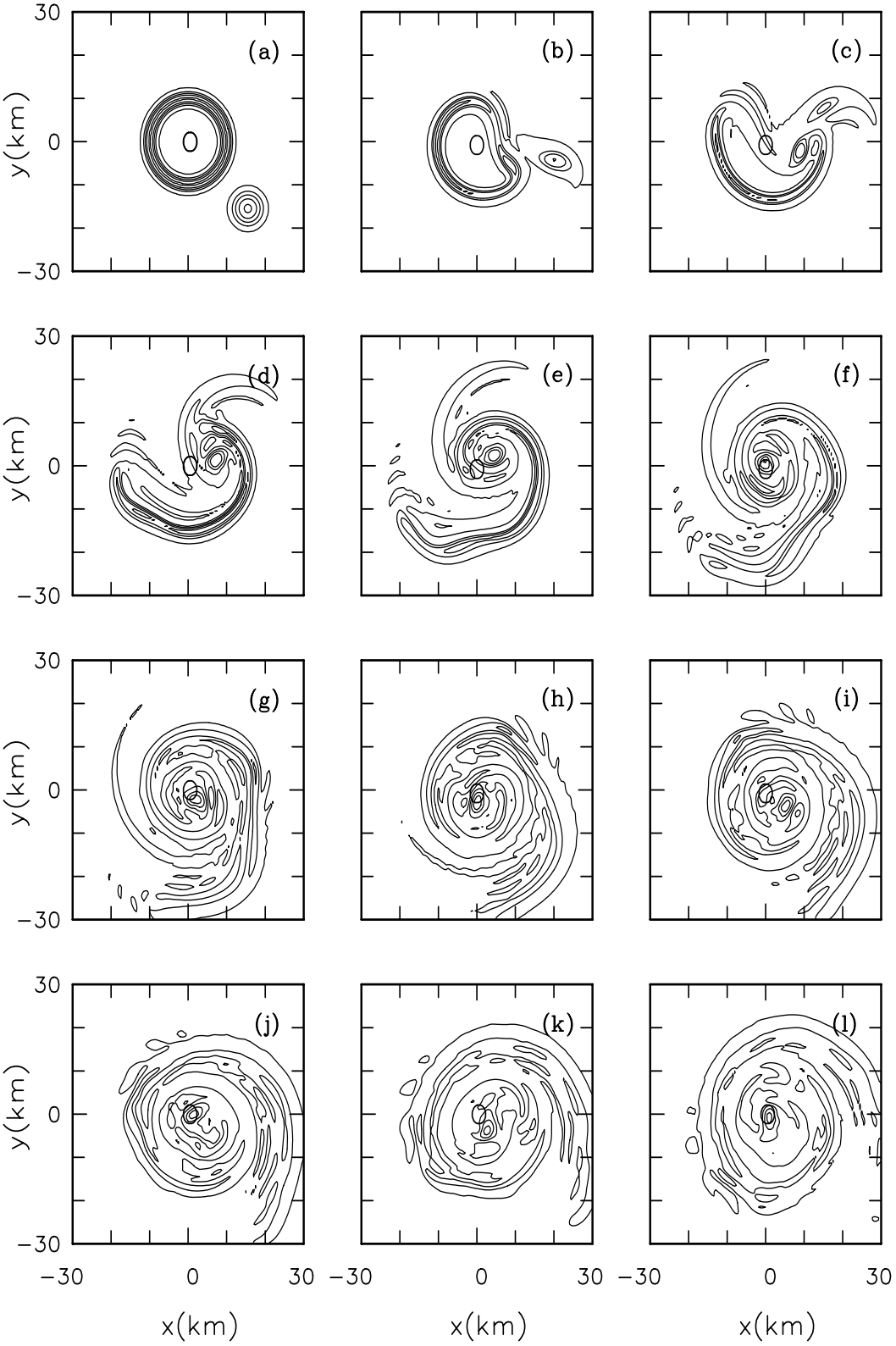


**Fig. 8.** Temporal changes of the vorticity field $\xi(x, y)$ in Expt. 4. The outmost peripheral contour of the vortex is $5.0\times10^{-4}$ s$^{-1}$, and the contour interval is $50.0\times10^{-4}$ s$^{-1}$. The others are the same as Fig. 3.

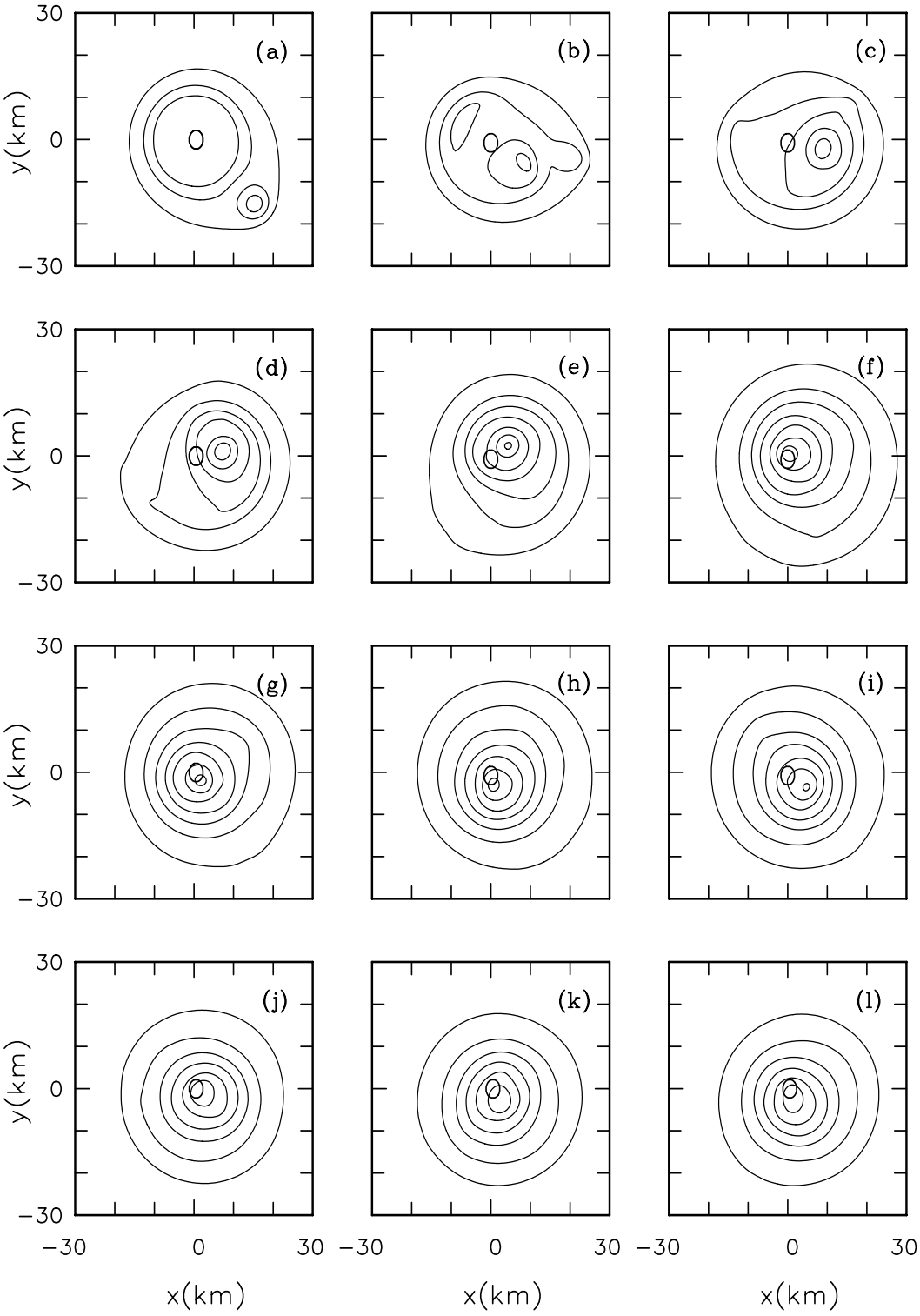


**Fig. 9.** Temporal changes of relative pressure field $p(x, y)$ in Expt. 4 at $t = 0$ (a), 10 (b), 20 (c), $\cdots$ , 110 (l) min. The contour interval is –4 hPa, and the others are the same as Fig. 3.

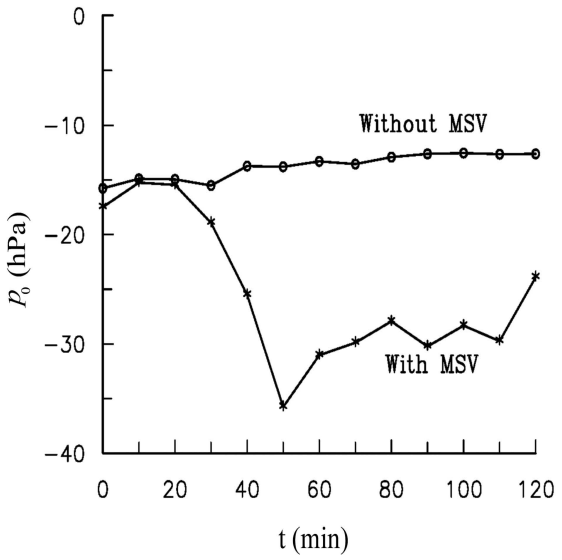


**Fig. 10.** Temporal variations of the relative pressure $p_0$ at the initial tropical cyclone center O in Expts. 3 (circles) and 4 (stars).

the eyewall of the tropical cyclone, the splitting of the zone means the rupture of the tropical cyclone circular eyewall and the transforming of the continuous eyewall into discontinuous ones. At $t = 60$ min, in addition to the four closed centers, a weak closed center appears at point O, several even smaller closed centers occur, and the flow pattern becomes complicated (Fig. 7g). Afterwards, the number of the smaller closed centers is decreased, the irregular extent of the peripheral contours is also reduced, but the feature of the discontinuous eyewalls of the quadrangle is still maintained (Figs. 7h–l).

In Experiment 3, at the initial time $t = 0$, the relative pressure at the initial tropical cyclone center $p_0$ is lower than –13 hPa; at $t = 10$ and 20 min, it is higher than –13 hPa; at $t = 30$ min, it is lower than –13 hPa again; and after $t = 40$ min, it remains higher than –13 hPa for the rest of the experiment. Correspondingly, the temporal evolution of the relative pressure field $p(x, y)$ in Experiment 3 also undergoes a transforming process from a pattern of a single closed center into multiple closed centers. And their spatial scales are larger at $t = 50$ min, and reduce gradually afterwards.

Experiment 4 implements the interaction of the tropical cyclone and the MSV. At the initial time $t = 0$, the center of the MSV is located at 21 km southeast of the tropical cyclone center (Fig. 8a), and at $t = 10$ min, it rotates anticlockwise to the ESE of the tropical cyclone center. In the process of the rotation, the MSV deforms and elongates, exhibiting a quasi-elliptic pattern, and the tropical cyclone vortex also deforms (Fig. 8b). At $t = 20$ min, the MSV continues its anticlockwise rotation as well as its elongation, and becomes a vorticity band; the high vorticity zone of the tropical cyclone circulation also further enfolds and elongates, with a small scale closed center in the vicinity of its east end and serrated perimeters on the northwest side of the tropical cyclone vortex (Fig. 8c). At $t = 40$ min, the main body of the original MSV merges with the small scale closed center near the east end of the high vorticity band, forming a vorticity accumulation area near the tropical cyclone center point O. The remainder of the original MSV forms a spiral band north of the vorticity accumulation area, and the west and central segments of the high vorticity band of the tropical cyclone circulation have evolved into two spiral bands south of the accumulation area (Fig. 8e). At $t = 50$ min, the vorticity accumulation area shows a typhoon-like spiral structure, and its center basically coincides with the tropical cyclone center point O (Fig. 8f). In comparison with the initial vorticity field, more vorticity has been transferred onto the tropical cyclone center point O, which will result in the intensification of the tropical cyclone. The vorticity flow entering point O consists of two parts: the vorticity of the MSV and the vorticity of the east segment of the high vorticity band of the tropical cyclone. Therefore it is the interaction of the MSV and tropical cyclone vortex that contributes to the accumulation of vorticity at the tropical cyclone center and the intensification of the tropical cyclone intensity. After $t = 50$ min, a typhoon-like spiral structure exists around the point O for the rest of the experiment, and its spiral bands rotate anticlockwise slowly (Figs. 8g–l).

In the initial relative pressure field $p(x, y)$, the relative pressure of the tropical cyclone center (point O) $p_0$ is lower than –13 hPa, and the MSV lies 21 km southeast of the tropical cyclone center, with a central relative pressure also being lower than –13 hPa (Fig. 9a). At $t = 10$ min, the MSV rotates anticlockwise and approaches the point O, while the relative pressure at the tropical cyclone center $p_0$ has increased to above –13 hPa (Fig. 9b). At $t = 30$ min, the center of the MSV has moved to a position 7 km due east of the point O, with a relative pressure lower than that at 21 km. Therefore, the relative pressure at the center of the MSV 7 km east of tropical cyclone center has further decreased, and its value has become lower than –25 hPa; the relative pressure at the tropical cyclone center (point O) $p_0$ correspondingly decreases to less than –13 hPa (Fig. 9d). At $t = 50$ min, the intensifying MSV center coincides basically with point O, and $p_0$ has decreased to less than –29 hPa (Fig. 9f). Phenomenally, after the interaction of the two vortices over the period from 0 to 50 min, the relative pressure at the

center of the tropical cyclone has decreased by about 16 hPa. Afterwards, the center of the MSV oscillates around point O for the rest of the experiment, and does not depart far from it (Figs. 9g–l). Thus, over the period from 50 to 110 min the relative pressure $p_0$ of the tropical cyclone center point O maintains a lower value to intensify the tropical cyclone intensity.

The temporal variations of $p_0$ in Experiments 3 and 4 (Fig. 10) demonstrate that the $p_0$ will slightly increase by 2 hPa over the time period from 0 to 120 min if there is no MSV interaction (Experiment 3) and $p_0$ will dramatically decrease by 14.1 hPa over the time period from 40 to 120 min if there is MSV interaction in the experiment (Experiment 4). The numerical experiments have shown that the interaction between the tropical cyclone and the MSV or the merging of an MSV into a tropical cyclone would lead to the intensification of the tropical cyclone.

## 5. Conclusion and discussion

Recently, the physical mechanism for the intensity change of tropical cyclones has become an active topic of tropical cyclone dynamics, and studying the propagation characteristics of vortex Rossby waves in the tropical cyclone circulation area has become one of the major research approaches (Möller and Montgomery, 1999, 2000; Montgomery and Kalenbach, 1997; Reasor and Montgomery, 2000).

The main working hypotheses of this paper are the following two points.

First, the condition of stationary tropical cyclone circulation was generally used in the existing papers (such as Möller and Montgomery, 1999, 2000; Montgomery and Kalenbach, 1997; Reasor and Montgomery, 2000), hence the vortex Rossby waves propagate in a stationary circular shearing basic flow. If an MSV initially lies at the maximum wind radius or in the outer region of a tropical cyclone, and if its vorticity propagates into the vicinity of the tropical cyclone center, then the tropical cyclone will be intensified. Here, the inward propagation of vorticity is a major reason for the intensification of the tropical cyclone. We consider that when a tropical cyclone and an MSV coexist, not only may the tropical cyclone affect the MSV, but the MSV may also affect the tropical cyclone with the process of its vorticity propagation. Therefore, the assumption of a stationary tropical cyclone circulation is invalid, and the vorticity propagation of the MSV should be analyzed under the condition of nonstationary tropical cyclone circulation.

Second, tropical cyclones have a diversity of different structures, but at least two types of structures can be distinguished. The first type is characterized by a tangential velocity $\overline{V}$ that increases rapidly with $r$ in the inner region of the tropical cyclone; e.g., in Hurricane Esther, the maximum tangential velocity $\overline{V}_{\max}$ reaches about 62.0 m s$^{-1}$, and its maximum wind radius $r_{\rm m}$ is about 21 km. The second type is characterized by a tangential velocity $\overline{V}$ that increases slowly with $r$ in the inner region of the tropical cyclone; e.g., in Hurricane Ginger, the maximum tangential velocity $\overline{V}_{\max}$ reaches about 34.0 m s$^{-1}$ and $r_{\rm m}$ is about 85 km (see Fig. 2.9b in Chen and Ding, 1979). Correspondingly, the maximum vorticity of Esther is 7.5 times that of Ginger. The former (latter) is denoted as a high (low) vorticity zonal structure. The interaction of vortices and its effect on the tropical cyclone intensity change are analyzed under the circumstances of two types of different tropical cyclone structures, in which the $\overline{\xi}_{\max}$ of the high vorticity zonal structure is 8.0 times that of the low vorticity zonal structure.

The two major conclusions of this paper are as follows:

First, under the condition of nonstationary tropical cyclone circulation, physical processes affecting the tropical cyclone intensity change include the inward propagation of the vorticity of the MSV and the effect of the process of merging vortices. Due to the interaction of the two vortices, the west and central segments of the high vorticity band of the tropical cyclone evolve into two spiral bands; and the merging of the east segment and the inward propagating vorticity of the MSV forms a new vorticity accumulation area where the vorticity maximum is larger than that of the initial tropical cyclone at the initial tropical cyclone center leading to the intensification of the tropical cyclone. This process is different from that of pure inward propagation of vorticity.

Second, the interaction of the tropical cyclone vortex of different structures with the MSV leads to different results. Under the condition of low vorticity zonal structure, the interaction leads to a pressure decrease of 3.8 hPa at the tropical cyclone center; while under the condition of high vorticity zonal structure, the interaction results in a pressure decrease of 14.1 hPa. The latter is 3.7 times the former. Therefore, the tropical cyclone structure also plays an important role in the intensity changes of tropical cyclone itself.

The dynamics of the tropical cyclone intensity change involves many physical processes, such as baroclinicity, diabatic heating, orographic forcing, interaction between the boundary layer and the free atmosphere, etc. (Wang et al., 1996; Gao, 2000; Meng et al., 2002; Yu, 2002). This research is performed within the framework of the advection dynamics of a 2D vortex, therefore the result obtained is preliminary.

Further studies are needed, especially to study the relative importance of these other processes as compared to the vortex interaction in the tropical cyclone intensity change.

***Acknowledgments.*** This work was jointly supported by the National Natural Science Foundation of China under Grant Nos. 40333028 and 40175019, and the Key Project of the Ministry of Science and Technology of China under Grant No. 2001DIA20026.

## REFERENCES

Chen Lianshou, and Ding Yihui, 1979: *An Introduction to the West Pacific Ocean Typhoons*. Science Press, Beijing, 491pp.

Chen Lianshou, and Luo Zhexian, 1995: Effect of the interaction of different scale vortices on the structure and motion of typhoon. *Adv. Atmos. Sci.*, **12**, 207–214.

Gao Shouting, 2000: The instability of the vortex sheet along the shear line. *Adv. Atmos. Sci.*, **17**, 525–537.

Gao Shouting, and Lei Ting, 2000: Streamwise vorticity equation. *Adv. Atmos. Sci.*, **17**, 339–347.

Kossin, J. P., and W. H. Schubert, 2001: Mesovortices, polygonal flow patters, and rapid pressure falls in hurricane-like vortices. *J. Atmos. Sci.*, **58**, 2196–2209.

Luo Zhexian, 1994: Study of effects of beta term and nonlinear advection on the structure of tropical cyclones. *Adv. Atmos. Sci.*, **11**, 391–398.

Luo Zhexian, 1999: Fractals of vortex and eddy perimeters. *Acta Meteorologica Sinica*, **57**, 330–337.

Meng Zhiyong, Chen Lianshou, and Xu Xiangde, 2002: Recent progress on tropical cyclone research in China. *Adv. Atmos. Sci.*, **19**, 103–110.

Möller, J. D., and M. T. Montgomery, 1999: Vortex Rossby waves and hurricane intensification in a barotropic model. *J. Atmos. Sci.*, **56**, 674–687.

Möller, J. D., and M. T. Montgomery, 2000: Tropical cyclone evolution via potential vorticity anomalies in a three-dimensional balance model. *J. Atmos. Sci.*, **57**, 3366–3387.

Montgomery, M. T., and R. J. Kalenbach, 1997: A theory for vortex Rossby-waves and its application to spiral bands and intensity changes in hurricanes. *Quart. J. Roy. Meteor. Soc.*, **123**, 435–465.

Ohnishi, H., 1991: Effect of the vortex structure on nonlinear beta drift. WMO/TD- No. 472, 43–51.

Reasor, P. D., and M. T. Montgomery, 2000: Low-wavenumber structure and evolution of the hurricane inner core observed by air-borne dual-Doppler radar. *Mon. Wea. Rev.*, **128**, 653–680.

Tian Yongxiang, and Luo Zhexian, 1994: Vertical structure of beta gyres and its effect on tropical cyclone motion. *Adv. Atmos. Sci.*, **11**, 43–50.

Wang Guomin, Wang Shiwen, and Li Jianjun, 1996: A bogus typhoon scheme and its application to a movable nested mesh model. *Adv. Atmos. Sci.*, **13**, 103–114.

Yu Zhihao, 2002: The spiral rain bands of tropical cyclone and vortex Rossby waves. *Acta Meteorologica Sinica,* **60**, 502–507.